PHYSICAL REVIEW B VOLUME 19, NUMBER 8 15 APRIL 1979

Quadrupole interaction in the scattering of H_2 from the surface of LiF: Rotational transitions

N. R. Hill

School of Physics, Georgia Institute of Technology, Atlanta, Georgia 30332

(Received 24 October 1978)

It is shown that when H_2 is scattered from the (001) surface of a LiF crystal, the quadrupole moments of the incident molecule interact with the electric field of the crystal to couple translational and rotational modes. This interaction causes rotational transition probabilities which are comparable in magnitude to those measured experimentally and to those calculated to result from other interaction mechanisms.

I. INTRODUCTION

A principal objective of molecular-beam diffraction studies of crystal surfaces[1] is to determine the interaction potential between the incident particle and the surface.[2] For many systems in which the incident particle is a light atom, the experimental elastic scattering intensities can be explained by calculations which assume a Van der Waals type interaction that arises from an induced-dipole, long-range attraction plus a hard-core, short-range repulsion.[3-7] In fact, in some cases it is possible to match experimental elastic scattering data while keeping only short-range repulsion,[8] even when modeling the repulsion as a corrugated hard wall.[9-11]

Several quantum-mechanical theories used for the scattering of atoms have been applied to the scattering of light diatomic molecules.[12-15] The calculations are used to describe not only the observed elastic scattering diffraction peaks,[16-18] but also to predict the intensity of beams consisting of molecules which have undergone rotational transitions upon scattering. These distinct beams were predicted by Logan,[19] who extended the analysis of Jackson and Howarth,[20] and were observed by Boato *et al.*[17] and Rowe and Ehrlich.[18] The mechanisms for inducing rotational transitions considered in past calculations stem from the oblong shape of the molecule[14,15,19] and the directional dependence of the molecular polarizability.[12] For ionic solids, however, there is an additional interaction which, so far, has been neglected in molecular-beam scattering theories, but is shown in this paper to contribute significantly to rotational transitions. This additional potential is the interaction of the lowest-order intrinsic multipole of H_2 (the quadrupole moment) with the electric field which is above an ionic crystal[21]:

$$V'(\vec{r},\theta,\phi) = -\frac{1}{6}\sum_{i,j} Q_{ij}(\theta,\phi)\,\frac{\partial E_j(\vec{r})}{\partial x_i}\,, \tag{1a}$$

$$Q_{ij} = \int (3x'_i x'_j - r'^2\delta_{ij})\,\rho(\vec{r}\,')\,d^3r'\,. \tag{1b}$$

Coordinates $(\vec{r},\theta,\phi)$ specify the position and orientation of the molecule. The primed coordinate system of (1b) has its origin at the position $\vec{r}$. The quadrupole interaction is known to be important in the physisorption of some molecules on ionic crystals.[22]

The purpose of this paper is to calculate interaction (1a) for the particular case of H_2 incident on LiF (Sec. II), and to estimate the magnitude of the rotational transitions it induces by causing a coupling between translational and rotational modes. It is shown that the transition probabilities caused by the above mechanism are comparable to those measured experimentally and to those calculated to result from other mechanisms (Sec. III). The rotational transitions are calculated to first order, using a flat hard wall, and a corrugated hard wall as zero-order potentials. Contributions to rotational transitions due to the oblong shape and the directional dependence of the polarizability of H_2 are not included, thereby isolating the effect of the interaction $V'(\vec{r},\theta,\phi)$ given in Eq. (1a).

II. QUADRUPOLE INTERACTION

The first task is to calculate the electric field resulting from crystal ions at observation points above the surface. Figure 1 illustrates a (010) section

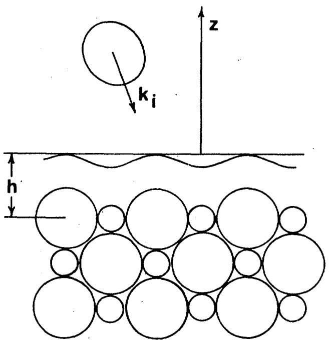

FIG. 1. H_2 incident on the (001) face of LiF. The flat, hard wall coincides with the plane $z=0$. The corrugated, hard wall is also shown.

of a LiF crystal with a (001) surface. The centers of the ions in the surface layer lie in the plane $z=-h$. The plane $z=0$ coincides with the flat, hard wall. One can calculate the potential at points with $z>0$ by beginning with the equation

$$\phi(\vec{r})=\int \frac{\rho(\vec{r}\,')}{|\vec{r}-\vec{r}\,'|}\, d^3r' \tag{2}$$

for a charge density distributions $\rho(\vec{r}\,')$. Denoting projections of three-dimensional vectors on to a plane parallel to the surface by upper case letters, e.g., $\vec{r}=(\vec{R},z)$, the Fourier transform of $1/|\vec{r}-\vec{r}\,'|$ in directions parallel to the surface is[23]

$$\frac{1}{|\vec{r}-\vec{r}\,'|}=\frac{1}{2\pi}\int d^2K\,\frac{e^{-\gamma|z-z'|}}{\gamma}\, e^{i\vec{K}\cdot(\vec{R}-\vec{R}\,')}, \tag{3}$$

with $\gamma=|\vec{K}|=(K_x^2+K_y^2)^{1/2}$. For $z>0$, one then gets

$$\phi(\vec{r})=\frac{1}{2\pi}\int d^2K\,\frac{e^{-\gamma z}}{\gamma}\, e^{i\vec{K}\cdot\vec{R}} \times\int d^3r'\,\rho(\vec{r}\,')e^{\gamma z'}e^{-i\vec{K}\cdot\vec{R}\,'}\,. \tag{4}$$

To reduce the expression for $\phi(\vec{r})$ further, it is now assumed that $\rho(\vec{r}\,')=\rho(\vec{r}\,'+\vec{l})$ where $\vec{l}$ is a lattice vector, and where $\vec{r}\,'$ and $\vec{r}\,'+\vec{l}$ are both points within the semi-infinite crystal. First, this assumes that the charge distribution in a unit cell next to the surface is the same as the distribution in a bulk unit cell, i.e., a semi-infinite, truncated-bulk model. This is a good approximation for an ionic crystal. Secondly, it supposes that phonon displacements of ions from their equilibrium positions can be ignored. This second point is discussed in the Appendix.

Fundamental lattice vectors are chosen in the $(1,1,0)$, $(\bar{1},1,0)$, and $(0,0,1)$ directions (see Fig. 2): $\vec{b}_x=(a/\sqrt{2})(1,1,0)$, $\vec{b}_y=(a/\sqrt{2})(\bar{1},1,0)$, and $\vec{b}_z=\sqrt{2}a(0,0,1)$. For LiF, the lattice constant is $a=2.84$ Å. This set is selected because $\vec{b}_x$ and $\vec{b}_y$ correspond to the usual choice for describing the surface of LiF. One can now reduce the second integral in (4) to

$$\begin{aligned}\int d^3r'\,\rho(\vec{r}\,')e^{\gamma z'}e^{-i\vec{K}\cdot\vec{R}} &=\sum_{\vec{l}} e^{\gamma l_z-i\vec{K}\cdot\vec{L}}\int_{\substack{\text{unit}\\ \text{cell}}} d^3r'\,\rho(\vec{r}\,')e^{\gamma z'}e^{-i\vec{K}\cdot\vec{R}\,'}\\ &=G^2{\sum_{\alpha,\beta}}'\frac{\delta(K_x-G\alpha)\delta(K_y-G\beta)}{1-e^{-\gamma_{\alpha,\beta}a\sqrt{2}}}\\ &\quad\times\int_{\substack{\text{unit}\\ \text{cell}}} d^3r'\,\rho(\vec{r}\,')e^{\gamma_{\alpha,\beta}z'}e^{-iG(\alpha x'+\beta y')},\end{aligned} \tag{5}$$

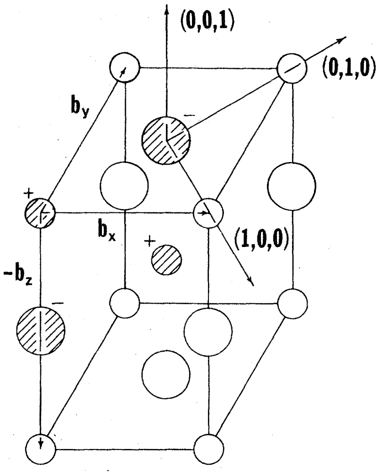

FIG. 2. Unit cell. The fundamental lattice vectors are chosen to be $\vec{b}_x$, $\vec{b}_y$, and $\vec{b}_z$; the corresponding set of basis ions is shaded. The length of $\vec{b}_x$ and $\vec{b}_y$ is $a=2.84$ Å; the length of $\vec{b}_z$ is $\sqrt{2}a=4.016$ Å.

where $G=2\pi/a$, $\gamma_{\alpha,\beta}=G(\alpha^2+\beta^2)^{1/2}$,

$$\vec{l}=(\vec{L},l_z)=m_x\vec{b}_x+m_y\vec{b}_y+m_z\vec{b}_z\,,$$

$m_z\leq 0$, and $\int_{\text{unit cell}}$ denotes integration over one unit cell next to the surface. The summation over α and β extends over all integers except $\alpha=\beta=0$.

The charge distribution is described by locating point charges having the magnitude of electronic charge $|e|$ at the positions of the ions. For the unit cell given by the present choice of lattice vectors (see Fig. 2), the charge distribution is

$$\begin{aligned}\rho(\vec{r})=|e|[&\delta(x)\delta(y)\delta(z+h)\\ &+\delta(x-a/2)\delta(y-a/2)\delta(z+h+a/\sqrt{2})\\ &-\delta(x-a/2)\delta(y-a/2)\delta(z+h)\\ &-\delta(x)\delta(y)\delta(z+h+a/\sqrt{2})]\,.\end{aligned} \tag{6}$$

This distribution assumes that the crystal bonds are purely ionic, and ignores the departure from this distribution caused by the bonds actually having a covalent contribution. LiF is, in fact, almost entirely ionic,[24] so this should be a good approximation. Substituting Eqs. (5) and (6) into (4) gives

$$\phi(\vec{r})={\sum_{\alpha,\beta}}'\frac{A_{\alpha,\beta}}{\gamma_{\alpha,\beta}^2}\, e^{iG(\alpha x+\beta y)}e^{-\gamma_{\alpha,\beta}z}, \tag{7a}$$

$$A_{\alpha,\beta}=\frac{|e|G^2}{2\pi}\,\frac{1-e^{-\gamma_{\alpha,\beta}a/\sqrt{2}}}{1-e^{-\gamma_{\alpha,\beta}\sqrt{2}\,a}}\, e^{-\gamma_{\alpha,\beta}h}\gamma_{\alpha,\beta}[1-(-1)^{\alpha+\beta}]. \tag{7b}$$

From this potential, one obtains the symmetric tensor

$$\left(\frac{\partial E_j}{\partial x_i}\right)={\sum_{\alpha,\beta}}'A_{\alpha,\beta}(G/\gamma_{\alpha,\beta})^2e^{iG(\alpha x+\beta y)}e^{-\gamma_{\alpha,\beta}z}\begin{pmatrix}\alpha^2 & \alpha\beta & i\alpha(\alpha^2+\beta^2)^{1/2}\\ \alpha\beta & \beta^2 & i\beta(\alpha^2+\beta^2)^{1/2}\\ i\alpha(\alpha^2+\beta^2)^{1/2} & i\beta(\alpha^2+\beta^2)^{1/2} & -(\alpha^2+\beta^2)\end{pmatrix}. \tag{8}$$

The orientation of the molecule is specified by coordinates (θ, ϕ), and the molecular symmetry axis is parallel to the z axis when $\theta = 0$. For $\theta = 0$ the value of the Q_{33} elements of the quadrupole moment [Eq. (1b)] is given by McLean and Yoshimine.[25] Cylindrical symmetry about the z axis for $\theta = 0$ implies $Q_{11} = Q_{22} = -\frac{1}{2} Q_{33}$ and $Q_{ij} = 0$, $i \neq j$.[21] The matrix can then be transformed to a general (θ, ϕ) to obtain

$$Q_{ij}(\theta, \phi) = \Theta\left(\frac{6\pi}{5}\right)^{1/2} \begin{pmatrix} Y_{2,2} + Y_{2,-2} - (2/3)^{1/2} Y_{2,0} & (Y_{2,2} - Y_{2,-2})/i & -(Y_{2,1} - Y_{2,-1}) \\ (Y_{2,2} - Y_{2,-2})/i & -(Y_{2,2} + Y_{2,-2} + (2/3)^{1/2} Y_{2,0}) & -(Y_{2,1} + Y_{2,-1})/i \\ -(Y_{2,1} - Y_{2,-1}) & -(Y_{2,1} + Y_{2,-1})/i & (8/3)^{1/2} Y_{2,0} \end{pmatrix}, \tag{9}$$

where the $Y_{l,m} = Y_{l,m}(\theta, \phi)$ are spherical harmonics. The value of the constant is $\Theta = 6.18 \times 10^{-27}$ esu cm^2.[25]

Equations (1a), (8), and (9) result in the interaction

$$\begin{aligned} V'(\vec{r}, \theta, \phi) = & -\Theta\left(\frac{\pi}{30}\right)^{1/2} \\ & \times \sum_{\alpha,\beta}{}' A_{\alpha,\beta} e^{iG(\alpha x + \beta y)} e^{-\gamma_{\alpha,\beta} z} \\ & \times [e^{i2\xi} Y_{2,2} + e^{-i2\xi} Y_{2,-2} \\ & - 2i(e^{i\xi} Y_{2,1} - e^{-i\xi} Y_{2,-1}) - \sqrt{6}\, Y_{2,0}], \end{aligned} \tag{10}$$

with $e^{i\xi} = (\alpha - i\beta)/(\alpha^2 + \beta^2)^{1/2}$.

III. ROTATIONAL TRANSITIONS

In this section, the rotational transitions caused by the quadrupole coupling between translational and rotational modes are calculated to first order using a flat hard wall as a zero-order potential, and treating potential (10) as a perturbation. These calculations are then extended to estimate the rotational transitions when the zero-order potential is a corrugated hard wall.

At energies of ~0.1 eV, typical of molecular scattering, the H_2 molecule can be considered a rigid rotor so that the zero-order Hamiltonian for points above the hard wall is

$$H_0 = p^2/2M + L^2/2I. \tag{11}$$

The moment of inertia I is given by

$$I = \tfrac{1}{4} M d^2, \tag{12}$$

where $d = 0.76$ Å is the average distance between the nuclei for H_2 in the ground state[26] and M is the total mass of the molecule. To find a solution of the complete Hamiltonian $H = H_0 + V'$ to first order in V', a Green's function Γ_0 for the zero-order Hamiltonian is constructed. It satisfies the equation

$$\begin{aligned} (H_0 - E_i)\Gamma_0(\vec{r}, \vec{r}', \theta, \theta', \phi, \phi') \\ = \delta(\vec{r} - \vec{r}')\delta(\phi - \phi')\delta(\cos\theta - \cos\theta'). \end{aligned} \tag{13}$$

The energy of the incident particle is

$$E_i = \hbar^2 k_i^2/2M + (\hbar^2/2I) l_i(l_i + 1), \tag{14}$$

k_i and l_i being the incident particle's wave-vector magnitude and its total angular-momentum quantum number. The solution ψ for the total Hamiltonian H obeys the Lippman-Schwinger equations,[27]

$$\psi = \psi_0 - \int \Gamma_0 V' \psi \, d\tau' . \tag{15}$$

The function ψ_0 is the zero-order wave function, the differential $d\tau' = d^3r' \, d(\cos\theta') \, d\phi'$, and the integral is over all points $\vec{r}'$ above the hard wall and all orientations (θ', ϕ') of the molecule. The functions ψ, ψ_0, and Γ_0 must all satisfy the boundary conditions of vanishing at the hard-wall and of being outgoing solutions. First-order results are obtained via the Born approximation of replacing ψ by ψ_0 on the right-hand side of (15).

Flat hard wall. First, the zero-order potential is modeled as a flat hard wall:

$$V_0(\vec{r}) = \begin{cases} 0, & z > 0 \\ \infty, & z < 0. \end{cases} \tag{16}$$

Although this potential does not include such important features of the real potential as the long-range attractive part and the corrugated shape of the repulsive part, it does allow a comparatively simple estimation of the coupling between translational and rotational modes caused by the quadrupole interaction when the incident H_2 molecule moves through the electric field above the surface. The hard-wall potential (16) also does not include crystal phonons in the scattering process and does not depend on the orientation of the molecule, so that the rotational transitions induced by interactions with the hard-wall can be ignored (see Ref. 14).

For a unit-amplitude, incident plane wave $e^{i\vec{k}_i \cdot \vec{r}}$, $\vec{k}_i = (\vec{K}_i, \kappa_i)$, the zero-order solution is

$$\psi_0(\vec{r},\theta,\phi)=e^{i\vec{K}_i\cdot\vec{R}}(e^{i\kappa_i z}-e^{-i\kappa_i z})Y_{l_i,m_i}(\theta,\phi)\,. \tag{17}$$

The Green's function Γ_0 is derived by an eigenfunction expansion:

$$\Gamma_0=\sum_{l,m}Y_{l,m}(\theta,\phi)Y^*_{l,m}(\theta',\phi')\,\frac{1}{(2\pi)^2}\times\int d^2K\,\frac{2}{\pi}\int_0^\infty d\kappa\,\frac{\sin\kappa z\,\sin\kappa z'\,e^{i\vec{K}\cdot(\vec{R}-\vec{R}')}}{E_{\vec{k},l}-E_i}\,,$$

$$E_{\vec{k},l}=(\hbar^2/2M)(K^2+\kappa^2)+(\hbar^2/2I)l(l+1)\,. \tag{18}$$

The κ integral can be performed by contour integration to yield the outgoing Green's function[28] for $z>z'$,

$$\Gamma_0=\frac{2M}{\hbar^2}\sum_{l,m}Y_{l,m}(\theta,\phi)Y^*_{l,m}(\theta',\phi')\,\frac{i}{8\pi^2}\times\int d^2K\,\frac{e^{i\kappa_{\vec{K},l}(z-z')}-e^{i\kappa_{\vec{K},l}(z+z')}e^{i\vec{K}\cdot(\vec{R}-\vec{R}')}}{\kappa_{\vec{K},l}}\,,$$

$$\kappa_{\vec{K},l}=+\{(k_i^2-K^2)+4/d^2[l_i(l_i+1)-l(l+1)]\}^{1/2}\,. \tag{19}$$

Using (10), (17), and (19), one can then calculate the Born approximation to (15):

$$\begin{aligned}\psi'(\vec{r},\theta,\phi)&=-\int\Gamma_0V'\psi_0\,d\tau'\\&=\sum_{l,m}\sum_{\alpha,\beta}{}'[\chi_{\alpha,\beta}(\kappa_i;\kappa_{\alpha,\beta,l})-\chi_{\alpha,\beta}(-\kappa_i;\kappa_{\alpha,\beta,l})]R_{\alpha,\beta}(l_i,m_i,l,m)\,e^{i\kappa_{\alpha,\beta,l}z}e^{i\vec{K}_{\alpha,\beta}\cdot\vec{R}}Y_{l,m}(\theta,\phi)\,,\end{aligned} \tag{20}$$

with $\vec{K}_{\alpha,\beta}=\vec{K}_i+G(\alpha\hat{i}+\beta\hat{j})$ and $\kappa_{\alpha,\beta,l}=\kappa_{\vec{K}_{\alpha,\beta},l}$. The function $\chi_{\alpha,\beta}$ is defined for arbitrary κ_1 and κ_2 as

$$\chi_{\alpha,\beta}(\kappa_1;\kappa_2)=\frac{2M}{\hbar^2}\,\Theta\left(\frac{\pi}{30}\right)^{1/2}A_{\alpha,\beta}\,\frac{i}{2\kappa_2}\left(\frac{1}{i(\kappa_1+\kappa_2)-\gamma_{\alpha,\beta}}-\frac{1}{i(\kappa_1-\kappa_2)-\gamma_{\alpha,\beta}}\right), \tag{21}$$

and the $R_{\alpha,\beta}$ is defined, using $3j$ symbols,[29] as

$$\begin{aligned}R_{\alpha,\beta}(l_i,m_i,l,m)=(-1)^m\left(\frac{5(2l+1)(2l_i+1)}{4\pi}\right)^{1/2}\begin{pmatrix}l&l_i&2\\0&0&0\end{pmatrix}\Bigg\{&e^{i2\xi}\begin{pmatrix}l&l_i&2\\-m&m_i&2\end{pmatrix}+e^{-i2\xi}\begin{pmatrix}l&l_i&2\\-m&m_i&-2\end{pmatrix}\\&-2i\left[e^{i\xi}\begin{pmatrix}l&l_i&2\\-m&m_i&1\end{pmatrix}-e^{-i\xi}\begin{pmatrix}l&l_i&2\\-m&m_i&-1\end{pmatrix}\right]\\&-\sqrt{6}\begin{pmatrix}l&l_i&2\\-m&m_i&0\end{pmatrix}\Bigg\}\,.\end{aligned} \tag{22}$$

For $l_i=m_i=0$, Eq. (22) reduces to

$$R_{\alpha,\beta}(0,0,l,m)=(\delta_{l,2}/\sqrt{4\pi}),[e^{i2\xi}\delta_{m,2}+e^{-i2\xi}\delta_{m,-2}-2i(e^{i\xi}\delta_{m,1}-e^{-i\xi}\delta_{m,-1})-\sqrt{6}\,\delta_{m,0}]\,.$$

The transition probability $P(\alpha,\beta,l_i\to l)$ of emerging in the diffracted beam (α,β) with total-angular-momentum quantum number l is obtained by averaging the beam amplitudes over m_i and summing them over m, and including a kinematic flux factor,[14]

$$P(\alpha,\beta,l_i\to l)=\left|\frac{\kappa_{\alpha,\beta,l}}{\kappa_i}\right|\frac{1}{2l_i+1}\sum_{m,m_i}|B_{\alpha,\beta}(l_i,m_i,l,m)|^2\,, \tag{23a}$$

$$\begin{aligned}B_{\alpha,\beta}(l_i,m_i,l,m)&=[\chi_{\alpha,\beta}(\kappa_i;\kappa_{\alpha,\beta,l})-\chi_{\alpha,\beta}(-\kappa_i;\kappa_{\alpha,\beta,l})]\\&\quad\times R_{\alpha,\beta}(l_i,m_i,l,m)\,.\end{aligned} \tag{23b}$$

These transition probabilities are significant only when $|\alpha|+|\beta|=1$; the factor $A_{\alpha,\beta}$ contained in $\chi_{\alpha,\beta}$ is zero or very small for other α and β owing to its dependence on $1-(-1)^{\alpha+\beta}$ and $e^{-\gamma_{\alpha,\beta}h}$ [see Eq. (7b)].

Some significant transition probabilities $P(\alpha,\beta,l_i\to l)$ are shown in Table I for several angles of incidence. The important result is that the values of the rotational transition probabilities caused by the quadrupole interaction are significant, and are on the same order as those determined experimentally by Boato *et al.*,[17] and theoretically, using other interaction models, by Garibaldi *et al.*,[14] and Wolken.[12,13] The distance h between the plane containing the surface ions and the hard wall is taken in these calculations as 2.75 Å. Considering that the average radius of H_2 taken from H_2-H_2 potentials is about 1.4 Å,[30] and that a typical value of the radius of F^- is 1.33 Å,[31] the chosen value for h is reasonable. It is em-

TABLE I. Rotationally inelastic diffraction probabilities $P(\alpha,\beta,l_i\rightarrow l)\times 10^3$ caused by the quadrupole interaction between H_2 and LiF with the zero-order potential modeled as a flat hard wall. The H_2 beam is incident at various angles θ_i in the $\langle 110\rangle$ azimuth. The incident wave vector is $k_i = 8.17$ Å^{-1}; the distance between the hard wall and the first layer of ions is $h = 2.75$ Å.

$(\alpha,\beta,l_i\rightarrow l)$ \ θ_i	5°	15°	30°	45°	60°
$(1,0,0\rightarrow 2)$	6.1 (3.5 [a])	2.8	···	···	···
$(\bar{1},0,0\rightarrow 2)$	10 (4.5 [a])	16	28 (4.0 [a])	50	55 (15 [a])
$(1,0,2\rightarrow 0)$	4.2 (0 [a])	5.9	10 (0.5 [a])	19 (2 [a])	41 (3 [a])
$(\bar{1},0,2\rightarrow 0)$	3.1	2.3	1.4	0.9	0.5

[a] Experimental values from Ref. 17.

phasized, though, that the representative value of h may be somewhat different. Since the rotational transition probabilities depend strongly on h, through the factor $e^{-\gamma_{\alpha,\beta}h}$ [see Eq. (7b)], changing h by an amount $\pm\Delta h$ results in the transition probabilities given in Table I being scaled by the factor $e^{\mp 2G\Delta h}$. (For all significant Fourier components in Eq. (7), those with $|\alpha|+|\beta|=1$, one has $\gamma_{\alpha,\beta}=G=2.21$ Å^{-1}.) Thus, if h is decreased to 2.5 Å, the values in Table I should be scaled by a factor of 3.0, and if h is increased to 3.0 Å, the values should be scaled by 0.33. Even in the latter case, the quadrupole interaction remains significant.

Corrugated hard wall. Although the results for the flat, hard wall show that the quadrupole interaction is significant, they predict appreciable transitions only into rotationally inelastic diffraction beams for which $|\alpha|+|\beta|=1$. Experimentally, appreciable transitions into other rotationally inelastic beams are observed.[17] The quadrupole interaction will contribute to these other beams if a more realistic corrugated shape is included for the hard wall.

One is immediately faced with the difficult problem of finding a Green's function Γ_0 which satisfies the boundary conditions of vanishing for points on the corrugated surface. If, however, the object is just to find results to the right order of magnitude, one can argue from the results for a flat, hard wall as follows.

Note that

$$\chi_{\alpha,\beta}(\kappa_i,\kappa_{\alpha,\beta,l})R_{\alpha,\beta}(l_i,m_i,l,m)$$

in Eq. (20) describes the coupling of a state $\exp[i(\vec{K}_i\cdot\vec{R}+\kappa_i z)]\,Y_{l_i,m_i}(\theta,\phi)$ to the state $\exp[i(\vec{K}_{\alpha,\beta}\cdot\vec{R}+\kappa_{\alpha,\beta,l}z)]Y_{l,m}(\theta,\phi)$. This coupling is caused by the quadrupole interaction as the H_2 molecule moves through the electric field above the surface. This interaction is not expected to depend greatly on the exact shape of the surface. Therefore, an estimate of rotational transitions can be obtained for the corrugated, hard wall by again using the same product $\chi_{\alpha,\beta}R_{\alpha,\beta}$, defined by Eqs. (21) and (22), to describe couplings between states. Specifically, since the hard-wall potential is not a function of θ and ϕ, the Rayleigh hypothesis[32] can be used to write the zero-order solution as

$$\psi_0(\vec{r},\theta,\phi) = \Big(e^{i\vec{k}_i\cdot\vec{r}} + \sum_{\mu,\nu} F_{\mu,\nu}\exp[i(\vec{K}_{\mu,\nu}\cdot\vec{R}+\kappa_{\mu,\nu,l_i}z)]\Big) \times Y_{l_i,m_i}(\theta,\phi)\,. \tag{24}$$

For the correct coefficients $F_{\mu,\nu}$, the wave function ψ_0 vanishes at the hard wall. Then in analogy with (17) and (20), the perturbation is approximately

$$\psi'(\vec{r},\theta,\phi) = \sum_{l,m}\sideset{}{'}\sum_{\alpha,\beta}\Big(\chi_{\alpha,\beta}(\kappa_i;\kappa_{\alpha,\beta,l})\exp[i(\vec{K}_{\alpha,\beta}\cdot\vec{R}+\kappa_{\alpha,\beta,l}z)] + \sum_{\mu,\nu}F_{\mu,\nu}\chi_{\alpha,\beta}(\kappa_{\mu,\nu,l_i};\kappa_{\mu+\alpha,\nu+\beta,l})\exp[i(\vec{K}_{\mu+\alpha,\nu+\beta}\cdot\vec{R}+\kappa_{\mu+\alpha,\nu+\beta,l}z)]\Big) \times R_{\alpha,\beta}(l_i,m_i,l,m)Y_{l,m}(\theta,\phi)\,. \tag{25}$$

TABLE II. Rotationally inelastic diffraction probabilities $P(\mu', \nu', l_i \rightarrow l) \times 10^3$ caused by the quadrupole interaction between H_2 and LiF with the zero-order potential modeled as a corrugated wall. The plane of incidence is in the ⟨110⟩ azimuth. The values of the constant are $k_i = 8.17$ Å^{-1}, $h = 2.75$ Å, and $\zeta_0 = 0.25$ Å.

$(\mu', \nu', l_i \rightarrow l)$ \ θ_i	5°	15°	30°	45°	60°
$(0, 0, 0 \rightarrow 2)$	0.8 (7[a])	1.2	3.1	···	···
$(1, 0, 0 \rightarrow 2)$	5.1 (3.5[a])	3.7	···	···	···
$(\bar{1}, 0, 0 \rightarrow 2)$	6.3 (4.5[a])	8.1	12 (4.0[a])	14	4.7 (15[a])
$(0, 0, 2 \rightarrow 0)$	0.2	0.3	0.6	1.9 (2[a])	1.7 (3.5[a])
$(1, 0, 2 \rightarrow 0)$	3.0 (0[a])	3.3	3.4 (0.5[a])	6.8 (2[a])	26 (3[a])
$(\bar{1}, 0, 2 \rightarrow 0)$	2.7	2.4	2.2	2.8	4.3

[a] Experimental values from Ref. 17.

The coefficients $F_{\mu,\nu}$ can be determined by using the Kirchhoff approximation.[9,33]

$$F_{\mu,\nu} = -\frac{k_i^2 + |\kappa_i| \kappa_{\mu,\nu,l_i} - \vec{K}_i \cdot \vec{K}_{\mu,\nu}}{\kappa_{\mu,\nu,l_i}(\kappa_{\mu,\nu,l_i} + |\kappa_i|)} i^{\mu+\nu} \times \exp[i(|\kappa_i| + \kappa_{\mu,\nu,l_i})\zeta_0] \times J_\mu((|\kappa_i| + \kappa_{\mu,\nu,l_i})\zeta_0/2) \times J_\nu((|\kappa_i| + \kappa_{\mu,\nu,l_i})\zeta_0/2)\,. \tag{26}$$

The shape of the surface is (see Fig. 1)

$$\zeta(x, y) = -\tfrac{1}{2}\zeta_0(\cos Gx + \cos Gy + 2)\,. \tag{27}$$

The corrugation amplitude is taken, after Garibaldi *et al.*,[14] to be $\zeta_0 = 0.25$ Å. The total reflected intensity predicted by (26) was within 5% of unity for all incident angles less than 60°, and within 15% for 60°.

The transition probability $P(\mu', \nu', l_i \rightarrow l)$ of emerging in the diffracted beam (μ', ν') with total-angular-momentum quantum number l is now

$$P(\mu', \nu', l_i \rightarrow l) = \left|\frac{\kappa_{\mu',\nu',l}}{\kappa_i}\right| \frac{1}{2l_i + 1} \sum_{m, m_i} |B_{\mu',\nu'}(l_i, m_i, l, m)|^2 \tag{28a}$$

$$B_{\mu',\nu'}(l_i, m_i, l, m) = \left(\chi_{\mu',\nu'}(\kappa_i; \kappa_{\mu',\nu',l}) + \sum_{\mu,\nu} F_{\mu,\nu}\chi_{\mu'-\mu,\nu'-\nu}(\kappa_{\mu,\nu,l_i}; \kappa_{\mu',\nu',l})\right) \times R_{\mu'-\mu,\nu'-\nu}(l_i, m_i, l, m)\,. \tag{28b}$$

Tables II and III give the values of transition probabilities computed from Eqs. (28) for a number of incidence angles in the ⟨110⟩ and ⟨100⟩ azimuths. Again we find that they are comparable in magnitude to experimental values[17] and to those computed using different interaction models.[12-14]

TABLE III. Rotationally inelastic diffraction probabilities $P(\mu', \nu', l_i \rightarrow l) \times 10^3$ under the same conditions specified in Table II, except in the ⟨100⟩ azimuth.

$(\mu', \nu', l_i \rightarrow l)$ \ θ_i	5°	15°	30°	45°	60°
$(0, 0, 0 \rightarrow 2)$	0.8 (7[a])	1.2 (7[a])	2.9 (6[a])	···	···
$(\bar{1}, \bar{1}, 0 \rightarrow 2)$	1.2 (0[a])	1.1	1.2 (2.0[a])	2.2 (4.0[a])	4.0 (15[a], 24[b])
$(\bar{2}, \bar{2}, 0 \rightarrow 2)$	···	0.4 (0[a])	0.6	0.6 (0[a])	0.5 (2.5[a], 1.8[b])
$(0, 0, 2 \rightarrow 0)$	0.2	0.3 (0.5[a])	0.6 (1.5[a])	1.6	1.3 (5[a], 13[b])
$(1, 1, 2 \rightarrow 0)$	0.3 (0[a])	0.3 (0[a])	0.9 (0[a])	4.0 (1.0[a])	0.1 (3[a], 0.2[b])
$(\bar{1}, \bar{1}, 2 \rightarrow 0)$	0.2	0.2	0.3	0.4 (2[a])	0.6 (2.5[a], 20[b])
$(\bar{2}, \bar{2}, 2 \rightarrow 0)$	0.3 (1.2[a])	0.3 (1.6[a])	0.2 (0[a])	0.2 (0[a])	0.1 (0[a], 1.8[b])

[a] Experimental values from Ref. 17.

[b] Theoretical values from Ref. 14.

IV. CONCLUSIONS

This article shows that when H_2 is scattered from the surface of a LiF crystal, the quadrupole moments of the incident molecule interact with the electric field of the crystal ions to couple translational and rotational modes. This interaction causes significant rotational transitions, and indicates the need for a rigorous calculation using a detailed potential which combines the quadrupole interaction with other important surface-potential features like a long-range attractive part. In addition, the detailed potential should allow for other important mechanisms which cause rotational transitions, such as those stemming from the oblong shape of H_2 and the directional dependence of its polarizability.

LiF is the subject of the present calculation because the crystal bonds are almost entirely ionic, thereby allowing a straightforward calculation of the electric field. Experiments have also been carried out scattering H_2 from MgO (Ref. 18) and Ag,[34] and rotationally inelastic beams are observed. To determine the significance of the quadrupole interactions in these cases, it is necessary to combine the general approach of this article with a microscope calculations of the electric field above the surface of each of these crystals. Since crystal bonds of MgO are largely ionic,[24] the quadrupole interaction between H_2 and MgO is probably similar in magnitude to the values calculated for H_2 and LiF. The contribution of the above interaction mechanism for molecular scattering from a metal surface could be estimated using the charge distribution for a metal surface cell in Eq. (5), which when used in Eq. (4) yields the potential at observation points above the surface. Recent calculations of metal-surface electronic-charge densities[35] employ a jellium model to represent the charge of ionic cores. For the purpose of the theory presented in this paper, the detailed contributions due to the ionic cores should be included. In the case of metal surfaces, the uncertainties in the location of the repulsive part of the potential [see the discussion in Sec. III following Eq. (23b)], as well as the interaction potential in general, are greater than for ionic crystals.[1(a),(1c)]

ACKNOWLEDGMENTS

I would like to thank Professor U. Landman, Professor V. Celli, and Mr. D. MacMillen for helpful discussions. This work was supported by the U. S. DOE under contract No. EG-77-S-05-5489.

APPENDIX: THERMAL MOTION OF THE IONS

The calculation has ignored the displacements of the ions from their equilibrium positions caused by thermal motion. The following analysis, which closely resembles a calculation of the Debeye-Waller factor,[36,37] justifies the neglect of the thermal motion.

The charge distribution $\rho(\vec{r})$ throughout the crystal is written as a sum of contributions from the ions:

$$\rho(\vec{r}\,') = \sum_{\vec{l}} \sum_{s} \rho_s(\vec{r}\,' - \vec{r}_{\vec{l},s}) . \tag{29}$$

The second sum is over all of the ions in a unit cell. The charge distribution ρ_s is contributed by an individual ion labeled s. The position of an ion, including the thermal displacement $\vec{u}_{\vec{l},s}(t)$ is

$$\vec{r}_{\vec{l},s} = \vec{l} + \vec{r}_s + \vec{u}_{\vec{l},s}(t) .$$

The vector $\vec{r}_s$ is the position in the unit cell of ion s relative to the lattice point $\vec{l}$.

The second integral in (4) is now reduced to

$$\int d^3r'\,\rho(\vec{r}\,')e^{\gamma z' - i\vec{K}\cdot\vec{R}'}$$

$$= \sum_{s} \sum_{\vec{l}} e^{\gamma l_z - i\vec{K}\cdot\vec{L}} e^{F_s} \int_{\text{unit cell}} d^3r'\,\rho_s(\vec{r}\,' - \vec{r}_s) \times e^{\gamma z' - i\vec{K}\cdot\vec{R}'} . \tag{30}$$

Letting $\vec{u}_{\vec{l},s} = (\vec{U}, u_z)$, the exponential factor is

$$e^{F_s} \equiv e^{\gamma u_z - i\vec{K}\cdot\vec{U}}$$
$$= 1 + (\gamma u_z - i\vec{K}\cdot\vec{U}) + \tfrac{1}{2}\gamma^2 u_z^2 - \tfrac{1}{2}(\vec{K}\cdot\vec{U})^2 + \ldots . \tag{31}$$

The second term in the expansion describes a time-varying component of the electric field which, although averaging to zero, may act through interaction (1a) to couple crystal phonons to rotational modes of the H_2 molecule. This article, however, is focused on the coupling between the rotational and translational modes of the H_2 molecule caused by the time-averaged electric field of the crystal ions. Thus, time averaging (31) so that only even-powered terms remain,[36] we obtain

$$\langle e^{F_s}\rangle = \exp(\gamma^2\langle u_z^2\rangle - K_x^2\langle u_x^2\rangle - K_y^2\langle u_y^2\rangle) . \tag{32}$$

If one assumes isotropic vibration, i.e., $\langle u_x^2\rangle = \langle u_y^2\rangle = \langle u_z^2\rangle$, then $\langle e^{F_s}\rangle$ is unity because $\gamma^2 = K_x^2 + K_y^2$. This simply results from assuming that the average charge distribution caused by each vibrating ion is spherically symmetric about the equilibrium position. Actually, for the ions near the surface, which are most important in determining the field, $\langle u_z^2\rangle$ is larger than the other two components.[38] Nevertheless, with $\langle u_i^2\rangle^{1/2} \simeq 0.1$ Å,[36,37] and $\gamma = |\vec{K}| \simeq 2\pi/a = 2.2$ Å^{-1}, the terms in the exponent of (32) are individually small, ~0.05. Therefore, even with $\langle u_i^2\rangle \neq \langle u_j^2\rangle$, the value of $\langle e^{F_s}\rangle$ is near unity, so that Eqs. (29) and (30) reduce to (5) for the small Fourier components $\vec{K}$ of the field. For larger $\vec{K}$, the components of the field are very small because of the factor $e^{\gamma z'}$ in (30) so that the influence of thermal vibrations on these components does not significantly affect the total field.

---

[1] For recent reviews, see (a) M. W. Cole and D. R. Frankl, Surf. Sci. 70, 585 (1978); (b) F. O. Goodman, Crit. Rev. Solid State Sci. 7, 33 (1977); (c) U. Landman and G. G. Kleinman, *Surface and Defects Properties of Solids* (Chemical Society, London, 1977), Vol. 6, p. 1.

[2] C. Schwartz, M. W. Cole, and J. Pliva, Surf. Sci. 75, 1 (1978).

[3] C. E. Harvie and J. H. Weare, Phys. Rev. Lett. 40, 187 (1978).

[4] N. Garcia, F. O. Goodman, V. Celli, and N. R. Hill, Phys. Rev. B 19, 1808 (1979).

[5] G. Wolken, Jr., J. Chem. Phys. 58, 3047 (1973).

[6] A. Tsuchida, Surf. Sci. 14, 375 (1969).

[7] H. Chow and E. D. Thompson, Surf. Sci. 59, 225 (1976).

[8] K. J. McCann and V. Celli, Surf. Sci. 61, 10 (1976).

[9] U. Garibaldi, A. C. Levi, R. Spadacini, and G. E. Tommei, Surf. Sci. 48, 649 (1975).

[10] G. Boato, P. Cantini, U. Garibaldi, A. C. Levi, L. Mattera, and R. Spadacini, J. Phys. C 6, L394 (1973).

[11] N. Garcia, J. Ibanez, J. Solana, and N. Cabrera, Solid State Commun. 20, 1159 (1976).

[12] G. Wolken, Jr., J. Chem. Phys. 59, 1159 (1973).

[13] G. Wolken, Jr., J. Chem. Phys. 62, 2730 (1975); Chem. Phys. Lett. 21, 373 (1973).

[14] U. Garibaldi, A. C. Levi, R. Spadacini, and G. E. Tommei, Surf. Sci. 55, 40 (1976).

[15] F. O. Goodman and W. S. Liu, Surf. Sci. 49, 417 (1975). This work applies the theory of N. Cabrera, V. Celli, F. O. Goodman, and R. Manson, Surf. Sci. 19, 67 (1970).

[16] D. R. O'Keefe, J. N. Smith, Jr., R. L. Palmer, and H. Saltsburg, J. Chem. Phys. 52, 4447 (1970); D. R. O'Keefe, R. L. Palmer, H. Saltsburg, and J. N. Smith, Jr., J. Chem. Phys. 49, 5194 (1968).

[17] G. Boato, P. Cantini, and L. Mattera, J. Chem. Phys. 65, 544 (1976); Jpn. J. Appl. Phys. Suppl. 2, Part 2, 553 (1974).

[18] R. Grant Rowe and G. Ehrlich, J. Chem. Phys. 62, 735 (1975); 63, 4648 (1975).

[19] R. M. Logan, Mol. Phys. 17, 147 (1969).

[20] J. M. Jackson and A. Howarth, Proc. R. Soc. London, Ser. A 152, 515 (1935).

[21] J. D. Jackson, *Classical Electrodynamics*, 2nd ed. (Wiley, New York, 1975), p. 142.

[22] D. M. Young and A. D. Crowell, *Physical Adsorption of Gases* (Butterworth, Washington, D.C., 1962), p. 49.

[23] P. M. Morse and H. Feshbach, *Methods of Theoretical Physics* (McGraw-Hill, New York, 1953), p. 1256.

[24] J. C. Phillips and J. A. Van Vechten, Phys. Rev. Lett. 22, 705 (1969); J. C. Phillips, Phys. Today 23, 23 (1970).

[25] A. D. McLean and M. Yoshimine, J. Chem. Phys. 45, 3676 (1966). The definition of the quadrupole moment used by these authors is one half the value defined here in Eq. (1b) and in Ref. 21.

[26] W. Kolos and L. Wolniewics, J. Chem. Phys. 41, 3674 (1964).

[27] L. I. Schiff, *Quantum Mechanics*, 3rd ed. (McGraw-Hill, New York, 1968), p. 319.

[28] See Ref. 23, p. 823.

[29] A. Messiah, *Quantum Mechanics* (Wiley, New York, 1966), Vol. II, p. 1054.

[30] E. A. Mason and J. O. Hirschfelder, J. Chem. Phys. 26, 756 (1957).

[31] C. Kittel, *Introduction to Solid State Physics*, 4th ed. (Wiley, New York, 1971), p. 129.

[32] N. R. Hill and V. Celli, Phys. Rev. B 17, 2478 (1978).

[33] N. R. Hill and V. Celli, Surf. Sci. 75, 577 (1978).

[34] G. Boato, P. Cantini, and R. Tatarek, J. Phys. F 6, L237 (1976).

[35] N. D. Lang and W. Kohn, Phys. Rev. B 1, 4555 (1970).

[36] See Ref. 31, p. 84.

[37] J. M. Ziman, *Principals of the Theory of Solids*, 2nd ed. (Cambridge University, London, 1972), p. 62.

[38] B. C. Clark, R. Herman, and R. F. Wallis, Phys. Rev. 139, A860 (1965).